ELSEVIER

JPRAS
An International Journal of
Surgical Reconstruction
www.JPRASurg.com

Muscle-derived decellularised extracellular matrix improves functional recovery in a rat latissimus dorsi muscle defect model

CrossMark

Xiaoyu K. Chen [a,b], Thomas J. Walters [a,*]

[a] United States Army Institute of Surgical Research, Extremity Trauma and Regenerative Medicine Research Program, San Antonio, TX, USA
[b] Wake Forest Institute for Regenerative Medicine, Winston-Salem, NC, USA

Summary   *Purpose:* Craniofacial maxillary injuries represent nearly 30% of all battlefield wounds, often involving volumetric muscle loss (VML). The physical loss of muscle results in functional deficits and cosmetic disfigurement. Although surgical solutions are limited, advances in biomaterials offer great promise for the restoration of form and function following VML. The primary purpose of this study was to determine whether muscle function could be restored in a novel VML rat model using muscle-derived extracellular matrix (M-ECM).
Methods: Ten percent of the mass of the latissimus dorsi (LD) was excised. Three groups were examined: 1) no repair of defect (DEF), 2) repair with M-ECM and 3) sham (all procedures except muscle excision). Four and 8 weeks post-surgery, the isometric contractile properties of the LD were assessed *in situ* and selected histological properties were evaluated.
Results: The defect resulted in an initial reduction in peak isometric force (Po) of 30%. At 8 weeks the difference between DEF and sham was 20.5%. At the same time, M-ECM was only 8.4% below sham. Although the histological analysis revealed a narrow, but well-formed band of muscle running along the middle of the M-ECM, it was judged to be too small to account for the observed improvement in muscle force.
Conclusions: Repair of VML with M-ECM can dramatically improve muscle function independent of muscle regeneration by providing a physical bridge that accommodates force transmission

 * Corresponding author. United States Army Institute of Surgical Research, Extremity Trauma and Regenerative Medicine, Fort Sam Houston, San Antonio, 78676 TX, USA. Tel.: +1 210 539 2726; fax: +1 210 916 3877.
 E-mail addresses: thomas.walters@us.army.mil, dr.thomas.walters@gmail.com (T.J. Walters).

Report Documentation Page		*Form Approved* *OMB No. 0704-0188*

Public reporting burden for the collection of information is estimated to average 1 hour per response, including the time for reviewing instructions, searching existing data sources, gathering and maintaining the data needed, and completing and reviewing the collection of information. Send comments regarding this burden estimate or any other aspect of this collection of information, including suggestions for reducing this burden, to Washington Headquarters Services, Directorate for Information Operations and Reports, 1215 Jefferson Davis Highway, Suite 1204, Arlington VA 22202-4302. Respondents should be aware that notwithstanding any other provision of law, no person shall be subject to a penalty for failing to comply with a collection of information if it does not display a currently valid OMB control number.

1. REPORT DATE **01 DEC 2013**	2. REPORT TYPE **N/A**	3. DATES COVERED **-**

4. TITLE AND SUBTITLE	5a. CONTRACT NUMBER
Muscle-derived decellularised extracellular matrix improves functional recovery in a rat latissimus dorsi muscle defect model.	5b. GRANT NUMBER
	5c. PROGRAM ELEMENT NUMBER
6. AUTHOR(S) **Chen X. K., Walters T. J.,**	5d. PROJECT NUMBER
	5e. TASK NUMBER
	5f. WORK UNIT NUMBER
7. PERFORMING ORGANIZATION NAME(S) AND ADDRESS(ES) **United States Army Institute of Surgical Research, JBSA Fort Sam Houston, TX**	8. PERFORMING ORGANIZATION REPORT NUMBER
9. SPONSORING/MONITORING AGENCY NAME(S) AND ADDRESS(ES)	10. SPONSOR/MONITOR'S ACRONYM(S)
	11. SPONSOR/MONITOR'S REPORT NUMBER(S)

12. DISTRIBUTION/AVAILABILITY STATEMENT
Approved for public release, distribution unlimited

13. SUPPLEMENTARY NOTES

14. ABSTRACT

15. SUBJECT TERMS

16. SECURITY CLASSIFICATION OF:			17. LIMITATION OF ABSTRACT **UU**	18. NUMBER OF PAGES **9**	19a. NAME OF RESPONSIBLE PERSON
a. REPORT **unclassified**	b. ABSTRACT **unclassified**	c. THIS PAGE **unclassified**			

Standard Form 298 (Rev. 8-98)
Prescribed by ANSI Std Z39-18

across the injury site. This method of repair may provide an easily translatable surgical method for selected forms of VML.

Twenty-six percent of all battlefield injuries involve the face and cranium, affecting 2000 US Service Members in the current wars.[1] These injuries often involve volumetric loss of soft tissue, especially skeletal muscle, resulting in severe cosmetic deformities and debilitating functional loss.[2,3] Currently, repair of these injuries is limited to autologous muscle transfers which can involve significant donor-site morbidity. Therefore, clinicians and researchers have increasingly focussed on tissue engineering and regenerative medicine to provide solutions.

Repair of VML with biological scaffolds has shown promise in preclinical animal studies, as well as in a limited clinical report.[3] Biological scaffolds have been shown to influence repair by recruitment of endogenous progenitor cells to the site of injury.[4–6] Additionally, they have been shown to undergo rapid degradation and replacement with host tissue,[7,8] and have been associated with the presence of muscle tissue in experimental and clinical repair of skeletal,[9–12] cardiac,[13] oesophageal[14] and lower urinary tract muscles.[15] Experimental and clinical repair of VML has typically involved biological scaffolds from allogenic/ xenogenic sources, for example, small intestinal submucosa (SIS)[16,17] or porcine-derived acellular bladder matrix (UBM).[18] Evidence exists that homologous scaffolds may provide a better environment for constructive remodelling.[9] Thus for skeletal muscle repair, muscle-derived extracellular matrix (M-ECM) would be expected to provide an appropriate source for biological scaffold.

Skeletal muscles located in different areas of the body have different demands and may encounter different environments during regeneration. Thus, it is necessary to develop therapies for VML in preclinical models that approximate the physical and biological demands of distinct clinical indications. To this end, most preclinical VML models are designed to develop therapies for extremity[10,11] or abdominal muscle repair.[16] For the development of potential therapies for craniofacial muscle repair, a murine latissimus dorsi (LD) muscle model has been reported previously.[18,19] However, the mouse LD muscle is at least an order of magnitude smaller than the human equivalent. Performing *in vivo* or *in situ* functional measures are technically difficult and were not performed in these studies. Nevertheless, the analysis of function in the form of mechanical measurements is the best indicator of successful muscle repair.

To address these issues, we developed a rat LD model involving VML, which had the advantages of: 1) resembling many of the facial muscles architecturally (e.g., frontalis, levator labii superioris and platysma muscle) and 2) lending itself to neural-evoked *in situ* functional analysis.

The explicit goal of this article was to assess the ability of an allogeneic M-ECM to restore function in a preclinical model for repair of craniofacial VML as well as the potential mechanism that contributed to the repair.

Materials and methods

Animals

Adult male Sprague-Dawley rats or adult male Lewis rats weighing about 350 g at the time of surgery (Harlan Laboratories, Indianapolis, IN, USA) were housed in a vivarium approved by the American Association for the Accreditation of Laboratory Animal Care, and provided with food and water ad libitum.

LD muscle contractile properties

Contractile properties were determined *in situ* while animals were anaesthetised with 1.5–2.5% isoflurane. Assessment of isometric muscle contraction was performed as previously described[20] with modifications. Details of the experimental set-up and functional testing are described in Figure 1. Following functional measurements the muscle was excised, weighed and snap-frozen for histological analysis.

LD defect surgery

A separate study was performed to develop the muscle model and in order to determine the relationship of defect size to force reduction and to assure that self-repair did not take place. This is detailed in Figure 2. The defect size chosen for the main study was 8 mm × 12 mm. This represented approximately 10% of the total LD weight. It was verified that the defect was incapable of self-repair in adult male Sprague-Dawley rats (350–400 g, $n = 6$) that received the defect and were examined 4 weeks later.

The surgical procedure for creating the defect was as follows. While under anaesthesia, a 3-cm incision was made on the back of the animal to expose the lateral edge of LD. Two 8 mm × 12 mm holes were made through the LD using a biopsy punch tool (Acu-Punch, Acutderm, Inc, Ft. Lauderdale, FL, USA) inserted 1 cm from the distal portion of the LD and along the fist vessel along the posterior edge of the LD (Figure 2). The fascia was then closed with 5/0 Vicryl sutures, and the skin was closed with 4/0 Monomid sutures.

VML defect repair

To assess whether M-ECM can improve the functional repair of LD defect, a set of adult male Lewis rats (350–370 g) was randomly divided into three groups ($n = 6$/group). One group received the defect as previously described (DEF group). The second group received the same surgery, but
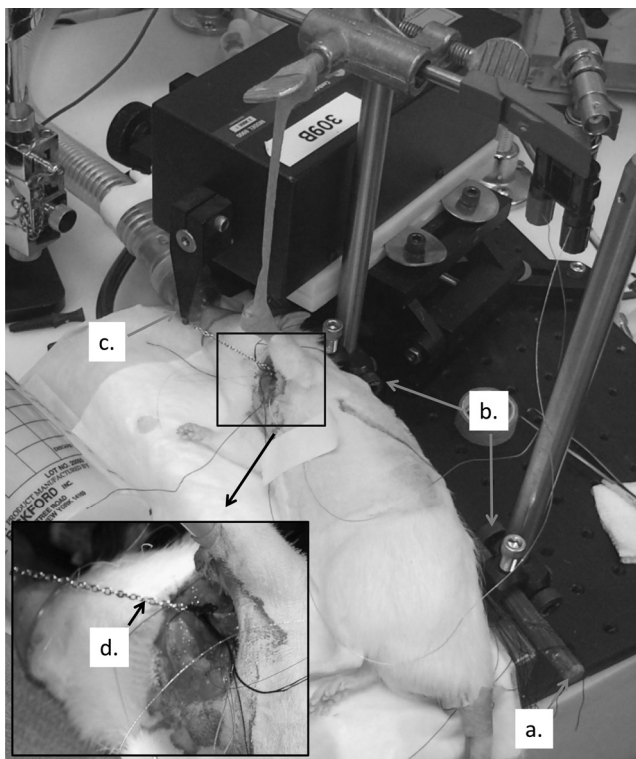
Figure 1 Experimental setup for measuring *in situ* mechanical properties of the LD. An incision was made from the base of the neck to approximately 1−2″ from the base of the tail. A ceramic rod was placed under the skin parallel to the spine and the rod was secured to the spine using a series of sutures around the spine and the rod. The skin was then wrapped around the rod and closed with surgical staples. The rod (a), with the spine secured to it, was then secured to an aluminum optical breadboard using standard mounting hardware (b). The distal tendon of the LD was then isolated and cut free of the insertion. The distal 1/3 of the muscle was carefully dissected free, taking care not to disrupt blood supply or injure the motor nerve. The distal tendon was attached to the lever arm (c) of the muscle lever system with a lightweight jeweler's chain (d) and secured with 4-0 silk suture (insert). Care was taken to maintain the *in vivo* orientation of the muscle. The isolated cut motor nerve was then threaded through a nerve cuff electrode.

the defect area was repaired with a piece of M-ECM of the same size (M-ECM group). The M-ECM was sutured to the LD using 6/0 Prolene suture with interrupted stitches. The third group went through the defect surgery but no defect was made. They served as sham controls (Sham group). Two months after surgery, muscle function was measured; the muscle was weighed and snap-frozen for histological analysis.

LD muscle decellularisation and characterisation

LD muscles were isolated from donor Lewis rats and decellularised as previously described in detail.[21] Briefly, LD muscles were freeze-thawed and soaked in deionised (DI) water for 72 h, then treated with 0.15% trypsin in
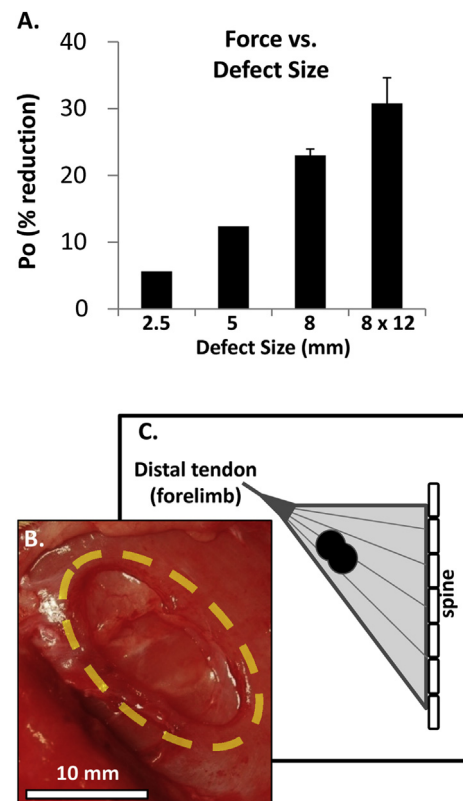

Figure 2 Composite image for model development. The relationship between the size of the defect and the resulting acute force deficit (A) was examined using progressively larger biopsy punches. An image of the exposed LD muscle shows the defect created using 2 overlapping excisions with an 8 mm punch (B). The anatomical location of the defect can be seen more clearly from the schematic diagram (C).

Dulbecco's Modified Eagle Medium(DMEM; Invitrogen, Carlsbad, CA, USA) at room temperature for 1 h. The muscles were then neutralised with 10% foetal bovine serum (FBS) in DMEM at 4 °C overnight and treated with 0.3% Triton X-100 (Fisher Scientific, Pittsburgh, PA, USA) with 2% ammonium hydroxide (Fisher Scientific, Pittsburgh, PA, USA) solution till the tissue was clear. The remaining triton was then rinsed off by phosphate-buffered saline. The complete decellularisation was confirmed by histology using haematoxylin and eosin stain (H&E), Masson's trichrome and 4',6-diamidino-2-phenylindole (DAPI) stains. The main composition of the M-ECM generated by the above method is collagen. For surgery, the M-ECM was sterilised with ultraviolet (UV) light overnight prior to implantation.

Functional analysis

Muscle functional tests were performed as previously described with modifications[20] using an Aurora muscle lever system (Aurora, Mod. 309B, ON, Canada). The muscle lever was controlled and data were acquired with a PC using a custom-designed LabView (National Instruments, Austin, TX, USA) based program. The nerve was stimulated using a physiological stimulator (A-M Systems, Model 2100

Isolated Pulse Stimulator, Carlsborg, WA, U.S.A.) at a stimulus intensity of two times the voltage required to elicit maximal peak twitch tension (Pt) and a pulse width of 100 μs. The muscle length adjusted until maximum tetanic tension (Po) was obtained under a stimulation frequency of 125 Hz, and all following measurements were made at this muscle length (Lo). The peak isometric forces at 1, 10, 20, 30, 40, 50, 60, 75, 100, 125, 150, 200 and 250-Hz stimulation were then recorded at 2-min intervals ($n = 6$) and forces were normalised as a percentage of force generated at 200 Hz.

Histology

Ten-micrometre cross sections were collected using a cryostat and stained with H&E stains for routine histology. For immunostains, tissue sections were stained for von-Willebrand factor(vWF),[21] desmin for muscle cells and MyoD for muscle progenitor cells.[20]

Statistical analysis

The Student t-test was used to evaluate differences in muscle force between injured LD and non-injured LD in model development. One-way analysis of variance (ANOVA) followed by least significant difference (LSD) post-hoc analysis were used to determine differences in muscle force and muscle weight among Sham, DEF and M-ECM repair groups at 2 months. A difference was considered significant when $P < 0.05$. All values are presented as mean $\pm$ standard error of the mean (SEM).

Results

Model development

Po increased over 4 weeks in both control and defect groups due to growth over this period (Figure 3B). The relative reduction in Po between control and defect groups went from 30% initially to 22% at 4 weeks. However, the absolute difference in Po was 2.3 and 2.2 N at 0 and 4 weeks, respectively. This suggests that growth of the existing muscle rather than muscle regeneration was responsible for the relative increase in Po over time. This is supported by a significant correlation between LD weight and Po at 4 weeks ($r^2 = 0.83$). Muscle weight remained significantly lower in the injured muscle compared to the control (Figure 3A). The weight deficit in injured muscle at 4 weeks was higher than that at the time of surgery possibly reflecting atrophy of the muscle fibres transected by the defect. However, visual inspection of photographs taken at time 0 and at 4 weeks did not show any appreciable difference in defect size to account for this difference. Taken together all the data clearly demonstrate that the defect did not undergo self-repair.

Muscle repair

After establishing the validity of the injury model in rat LD muscle, we investigated whether M-ECM could be used to surgically repair the injury and restore muscle function.
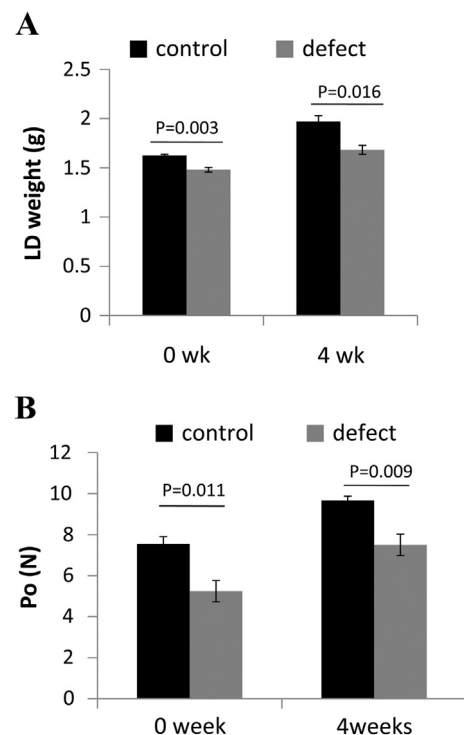

Figure 3 Muscle mass and muscle force at 0 and 4 weeks. The 8×12 defect caused significant decrease in muscle mass and muscle tetanic force (Po). A: LD muscle mass at 0 and 4 weeks showing muscle mass did not self-recover; B: LD muscle Po (125 Hz) at 0 and 4 weeks showing muscle function did not self-recover. The increase in muscle weight and absolute force resulted from animal growth during that time period.

Muscle function

Animal weights at the time of surgery were similar between groups and at the time of surgery and at 8 weeks (Table 1). LD muscle weights remained similar between DEF and M-ECM repair groups (1.28 $\pm$ 0.04 g and 1.28 $\pm$ 0.03 g, respectively), both of which were significantly lower than that in the sham group (Table 1). Compared to the sham controls, Po was 22% lower in the DEF group ($p < 0.05$) but only 8.7% lower in the M-ECM group ($p > 0.05$). The Po in M-ECM group was significantly higher than that in the DEF group (Figure 4A). The normalised Po (Ng^{-1} muscle) was significantly lower in DEF compared with that in the shams, but there was no difference between shams and M-ECM (Figure 4B). The force at any given frequency was statistically similar between sham and M-ECM, and was significantly less between sham and DEF at 75 Hz and above (Figure 4C). However, the normalised force–frequency curve ($P/Po \times 100$) showed no significant differences between the forces at any given frequency among the three groups, indicating that no qualitative changes took place in the remaining muscles (Figure 4D).

Histological analysis

At both 4 weeks (not shown) and 8 weeks, we observed that a thin transparent layer of connective tissue had formed within the defect (DEF group). The striated muscle beneath the defect could be easily seen (Figure 5A). The analysis of

Table 1 Animal weight and LD muscle weight.

Group	Animal weight at surgery (g)	Animal weight at 8 weeks post surgery (g)	Weight of excised muscle (g)	LD muscle weight (g)
Sham	360 ± 4	$422 + 6$	0	1.49 ± 0.06
DEF	355 ± 1	412 ± 4	0.130 ± 0.003	1.28 ± 0.04^a
M-ECM	355 ± 1	408 ± 5	0.132 ± 0.001	1.28 ± 0.03^a

^{a} Significantly different from Sham ($P < 0.05$).
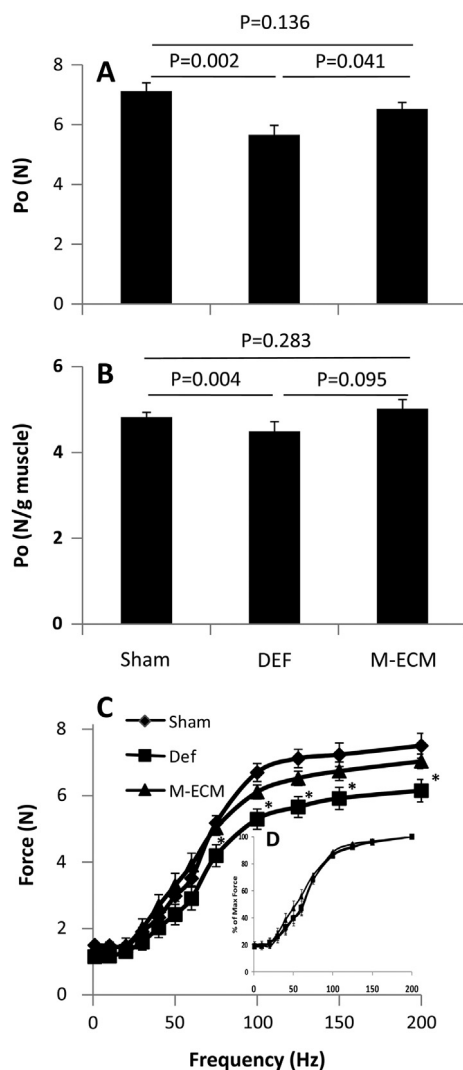
Figure 4 Repair with M-ECM resulted in a significant improvement in absolute maximal isometric force (Po) compared to DEF (no repair) (A). The absolute (A) and normalized Po (B) was not different from the Sham group (uninjured). In contrast, normalized Po was significantly reduced in DEF compared to Sham. The force (P) was significantly less in DEF at every frequency above 60 Hz (C) ($p < 0.05$); M-ECM displayed restoration of force at all frequencies. When P was expressed relative to Po, the curves were similar across groups (D).

the transparent layer using stains such as H&E, Masson's trichrome, desmin and collagen revealed that it was primarily composed of collagen with an absence of muscle cells (not shown). Physically, the layer was much thinner and more compliant compared to the M-ECM. By contrast, the M-ECM was well integrated with the host tissue by 8 weeks with regeneration of microvasculature throughout the entire M-ECM (Figure 5B). Microscopic examination of blood vessels within the M-ECM revealed that they were derived from adjacent LD muscle and grew in to the scaffold from all directions (Figure 4D). The connection between blood vessels within M-ECM and adjacent LD muscle was further proven by Indian ink perfusion (data not shown). No blood vessels were observed within the connective tissue formed in the DEF group (Figure 5C).

H&E sections showed that within the M-ECM, there was a narrow band of regenerating muscle fibres (Figure 5B and D). The width of this band was approximately 110 μm or 1/10th the thickness of intact LD (1056 μm; Figure 5A). The presence of muscle cells within the band was further confirmed with desmin immunostain (Figure 6E). However, the majority of the M-ECM did not contain muscle fibres. Scattered positive MyoD stain was observed throughout the M-ECM, suggesting the presence of muscle progenitor cells (Figure 6F). It was unclear if these progenitor cells could generate more muscle fibres given a longer period of time.

Discussion

Our study suggests that repair of VML using M-ECM results in significant improvements in muscle function in a rat model. A number of histologically based studies of repair of VML using a variety of scaffolds[12,22,23] or scaffold/cell combinations[24,25] have been published. These studies have used histological evidence of muscle regeneration, as an indication that the scaffolds have been successful. However, histological assessment correlates poorly with muscle function.[26] The magnitude of muscle regeneration in our study is consistent with other published reports wherein biological scaffolds are used in the repair of VML.[16,27] However, it is clear that the magnitude of functional recovery is in excess of what can be accounted for by the level of muscle regeneration observed. This underscores the importance of using muscle function as one of the primary outcome measures when assessing repairs of VML. In fact, VML is defined as "...traumatic or surgical loss of skeletal muscle with resultant functional impairment."[2] It is also noteworthy that functional
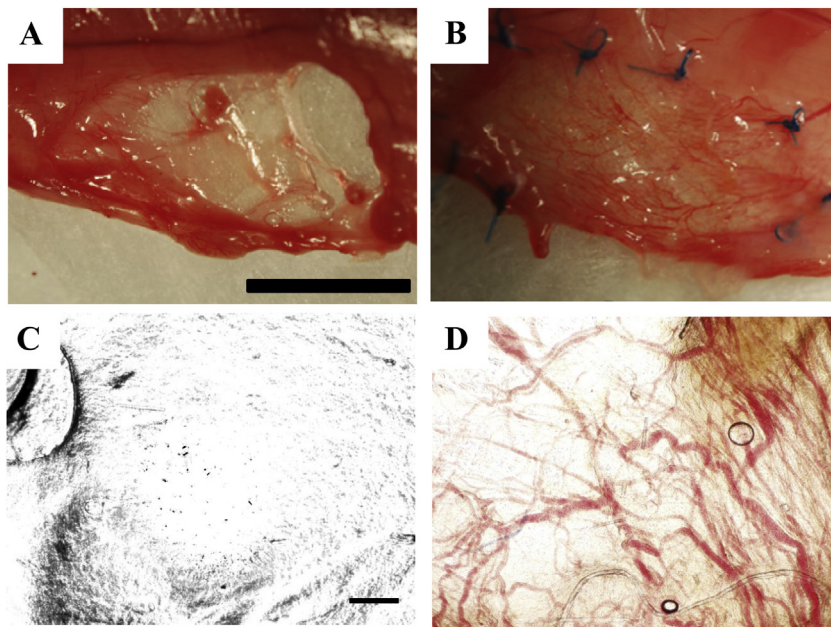
Figure 5 Representative images of DEF (A) and M-ECM repaired LD muscles (B) at 8 weeks after VML defect injury. Inspection of DEF (A) reveals a thin, white, layer of connective tissue largely devoid of vessels. In contrast M-ECM repair (B) resulted in a visibly well vascularized layer of tissue (outlined by intact sutures) that appears similar to the surrounding muscle and appears well integrated with the host tissue. The lack of vascularization seen in the thin white layer in (A) was confirmed in a microscopic image (C) from the same area, which appears as a featureless image. In contrast, a microscopic image of the repair with M-ECM (D) confirmed extensive vascularization within the implanted ECM. Scale bar in A-B = 1 cm, scale bar in C-D = 250 μm.

assessment was done *in situ*, leaving the neural and vascular supplies intact. Stimulating the motor nerve *in situ* has the added advantage of providing information that is more generalisable to *in vivo* conditions, in contrast to studies that assess muscle function *in vitro* (e.g., in an organ bath).

Successful repair of VML with a biological scaffold assumes that the scaffold itself will undergo rapid degeneration, followed by host-directed remodelling involving the recruitment of endogenous progenitor cells in to the implanted scaffold. In the present study, we observed the formation of a band of muscle fibres (stained positive for desmin) within the scaffold at 8 weeks postimplant. The width of this band is approximately 110 μm or 1/10th the thickness of intact LD (1056 μm) (Figure 6B and D). Assuming that the fibres present were functional, that is, innervated and able to generate force, we surmised that they would only account for a maximum 1/10th of the observed muscle contraction. A more plausible explanation for our finding of improved function is that the scaffold provided a bridge between the intact muscle fibres, providing a link for mechanical transmission of force across the defect area via a patch composed primarily of collagen.

In addition to providing physical continuity, the M-ECM supported rapid regeneration of the microvasculature (Figure 5D). The patency of the vascular network was confirmed using Indian ink perfusions (data not shown). The presence of an extensive vascular network can be reasonably expected to restore the blood flow on the opposing sides of the defect. It may also provide a route for the delivery of treatments, such as growth factors and stem cells in future studies.

Visual inspection of the repaired and unrepaired defects shows that the M-ECM allowed the LD to maintain its three-dimensional form (Figure 4B), providing an appearance similar to an uninjured muscle. This is important as it suggests that in addition to the ability of the M-ECM to restore function, it will also act as a stable filler. This feature may prove to be useful in reconstructive and aesthetic surgery.

There are a number of animal models for VML involving the extremities[10,21,28] and abdominal muscles.[16,24] Our focus was on the muscles of the craniofacial maxillary region. We therefore developed an animal model that approximates the flat parallel arrangement of many of the facial muscles (e.g., frontalis, levator labii superioris and Platysma muscle), yet converges onto a tendon to allow functional measurements. Also critical was the ability to isolate the motor nerve for neural stimulation of muscle activation. Interestingly, the physical size of the rat LD approximates many human facial muscles, making it more clinically relevant than the current LD murine models.[18] The defect created for our model involved the excision of ≈10% of the muscle mass, which resulted in a ≈30% reduction in force. This reduction in force may seem excessive relative to the size of the defect. However this can be explained by the fact that removal of muscle resulted in the inability to transmit force from (roughly) 1/3 of the muscle (Figure 6). By providing a mechanical bridge between the transected ends, the ability to transmit force was partially restored (Figure 7). Interestingly, at 8 weeks postinjury the difference in Po between sham and M-ECM was 8%, which may be accounted for by the 10% of muscle mass originally excised.
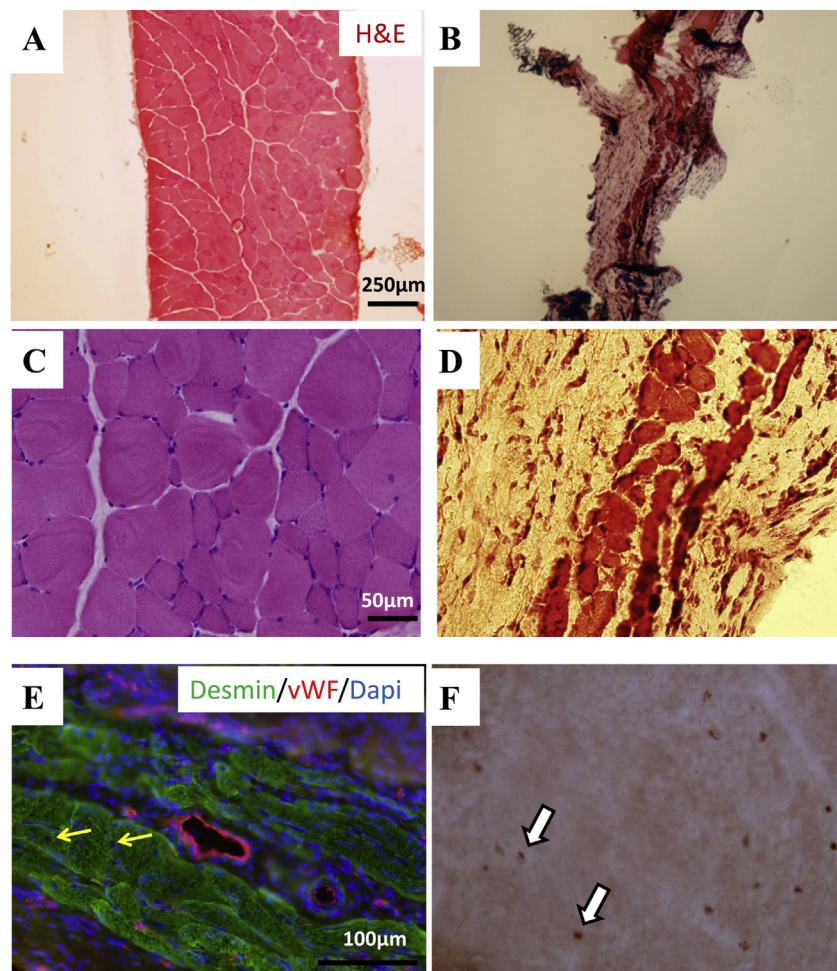
Figure 6 Micrographs of cross-sections of normal LD muscle (A,C) and M-ECM (B,D,E,F) at 8 weeks post injury. A thin band of muscle within the M-ECM is apparent in (B) and in the close-up view in (D); stained with H & E. Immunofluorescent staining in (E) for desmin (green cells) supports the existence of muscle cells in the band seen in the H & E stained sections. vWF staining reveals large vessels and capillaries within and outside the band of muscle (violet stained features). Cell nuclei are visible adjacent to muscle cells (blue dots, see yellow arrows for examples). A section of the ECM outside of the band of muscle shows scattered muscle precursor cells (see arrow for example) as indicated by MyoD staining (D). Scale bar in A-B = 1 cm, scale bar in C-D = 50 μm, scale bar in E-F = 100 μm.

Based on our results, bridging, not regeneration of muscle, was the main contributor of improved muscle function. This limits the utility of this method of repair to injuries with functional, intact muscle on opposing sides of the injury. Complete restoration of muscle function would still require the generation of a replacement muscle. The M-ECM used in the present investigation clearly provided an environment that fostered neo-muscle formation as indicated by an organised band of MyoD-stained cells (Figure 6B). It is possible that 8 weeks was insufficient for the full regenerative potential of the M-ECM to be realised. For example, Turner et al.[29] found that 6 months were required for partial muscle regeneration in a canine muscle/tendon excision model repaired with SIS. Valintin et al.[16] showed extensive neo-muscle formation after 6 months in a rat abdominal muscle defect model repaired with porcine SIS.

Although our evidence strongly suggests that muscle functional recovery is mainly due to bridging, this does not mean that any material can be used to bridge muscle defects. For example, inert prosthetic mesh, such as polypropylene mesh, has been used for repairing muscle defects. However, bridging defects with polypropylene mesh does not improve muscle function.[16] Similarly, repairing a VML in a mouse LD model using bladder-derived ECM did not improve functional recovery unless exogenous muscle progenitor cells were used.[18] This suggests that in order for the bridge to improve muscle function, the material must also be highly compatible with the host tissue. M-ECM showed superior compatibility to muscle tissue compared to many other materials as shown by the degree of regeneration and angiogenesis. M-ECM also supports muscle cell growth better than other types of ECMs.[9] In our preliminary study, neither functional recovery nor angiogenesis was observed using bladder-
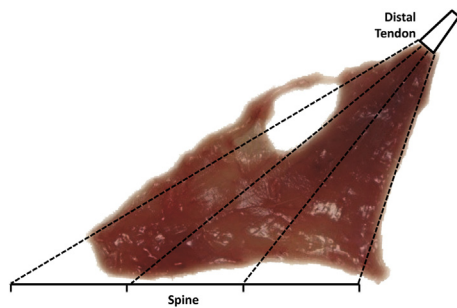
Figure 7 An excised LD muscle with defect. The proximal portion of the muscle (origin = spine) has been divided into equal thirds and vectors have been drawn to the distal tendon (hatch lines). From this it can be seen that the defect transects approximately 1/3 of the muscle, effectively eliminating the ability to transmit force across that portion the muscle. Repair with M-ECM provides a bridge between the transected portions of the muscle allowing the transmission of force to the distal tendon. Note also that this image explains how the removal of only 10% of the muscle mass causes a 30% reduction in force.

derived ECM to repair muscle defects in rat LD (data not shown).

Conflicts of interest

None.

Acknowledgements

References

1. Lew TA, Walker JA, Wenke JC, Blackbourne LH, Hale RG. Characterization of craniomaxillofacial battle injuries sustained by United States service members in the current conflicts of Iraq and Afghanistan. *J Oral Maxillofac Surg* 2010; **68**:3—7.

2. Grogan BF, Hsu JR. Volumetric muscle loss. *J Am Acad Orthop Surg* 2011;**1**(Suppl. 19):S35—7.

3. Mase Jr VJ, Hsu JR, Wolf SE, et al. Clinical application of an acellular biologic scaffold for surgical repair of a large, traumatic quadriceps femoris muscle defect. *Orthopedics* 2010;**33**:511.

4. Reing JE, Zhang L, Myers-Irvin J, et al. Degradation products of extracellular matrix affect cell migration and proliferation. *Tissue Eng Part A* 2008. http://dx.doi.org/10.1089/ten.tea.2007.0425.

5. Brennan EP, Tang XH, Stewart-Akers AM, Gudas LJ, Badylak SF. Chemoattractant activity of degradation products of fetal and adult skin extracellular matrix for keratinocyte progenitor cells. *J Tissue Eng Regen Med* 2008;**2**(18):491—8.

6. Beattie AJ, Gilbert TW, Guyot JP, Yates AJ, Badylak SF. Chemoattraction of progenitor cells by remodeling extracellular matrix scaffolds. *Tissue Eng* 2008. http://dx.doi.org/10.1089/ten.tea.2008.0162.

7. Gilbert TW, Stewart-Akers AM, Simmons-Byrd A, Badylak SF. Degradation and remodeling of small intestinal submucosa in canine Achilles tendon repair. *J Bone Joint Surg Am* 2007;**89**:621—30.

8. Gilbert TW, Stewart-Akers AM, Badylak SF. A quantitative method for evaluating the degradation of biologic scaffold materials. *Biomaterials* 2007;**28**:147—50.

9. Stern MM, Myers RL, Hammam N, et al. The influence of extracellular matrix derived from skeletal muscle tissue on the proliferation and differentiation of myogenic progenitor cells ex vivo. *Biomaterials* 2009;**30**(2):2393—8.

10. Merritt EK, Hammers DW, Tierney M, et al. Functional assessment of skeletal muscle regeneration utilizing homologous extracellular matrix as scaffolding. *Tissue Eng Part A* 2010;**16**:1395—405.

11. Merritt EK, Cannon MV, Hammers DW, et al. Repair of traumatic skeletal muscle injury with bone-marrow-derived mesenchymal stem cells seeded on extracellular matrix. *Tissue Eng Part A* 2010;**16**:2871—81.

12. Sicari BM, Agrawal V, Siu BF, et al. A murine model of volumetric muscle loss and a regenerative medicine approach for tissue replacement. *Tissue Eng Part A* 2012;**18**(19—20):1941—8.

13. Badylak SF, Kochupura PV, Cohen IS, et al. The use of extracellular matrix as an inductive scaffold for the partial replacement of functional myocardium. *Cell Transplant* 2006;**1**(Suppl. 15):S29—40.

14. Badylak SF, Vorp DA, Spievack AR, et al. Esophageal reconstruction with ECM and muscle tissue in a dog model. *J Surg Res* 2005;**128**:87—97.

15. Vaught JD, Kropp BP, Sawyer BD, et al. Detrusor regeneration in the rat using porcine small intestinal submucosal grafts: functional innervation and receptor expression. *J Urol* 1996;**155**:374—8.

16. Valentin JE, Turner NJ, Gilbert TW, Badylak SF. Functional skeletal muscle formation with a biologic scaffold. *Biomaterials* 2010;**31**:7475—84.

17. Turner NJ, Yates Jr AJ, Weber DJ, et al. Xenogeneic extracellular matrix as an inductive scaffold for regeneration of a functioning musculotendinous junction. *Tissue Eng Part A* 2010;**16**:3309—17.

18. Machingal MA, Corona BT, Walters TJ, et al. A tissue-engineered muscle repair construct for functional restoration of an irrecoverable muscle injury in a murine model. *Tissue Eng Part A* 2011;**17**:2291—303.

19. Corona BT, Machingal MA, Criswell T, et al. Further development of a tissue engineered muscle repair (TEMR) construct in vitro for enhanced functional recovery following

implantation in vivo in a murine model of volumetric muscle loss (VML) injury. *Tissue Eng Part A* 2012;**18**(11—12):1213—8.

20. Chen XK, Rathbone CR, Walters TJ. Treatment of tourniquet-induced ischemia reperfusion injury with muscle progenitor cells. *J Surg Res*;170:e65—e73.

21. Wu X, Corona BT, Chen X, Walters TJ. A standardized rat model of volumetric muscle loss injury for the development of tissue engineering therapies. *Bio Research Open Access* 2012;**1**:280—90.

22. Wolf MT, Daly KA, Reing JE, Badylak SF. Biologic scaffold composed of skeletal muscle extracellular matrix. *Biomaterials* 2012;**33**:2916—25.

23. Kin S, Hagiwara A, Nakase Y, et al. Regeneration of skeletal muscle using in situ tissue engineering on an acellular collagen sponge scaffold in a rabbit model. *Asaio J* 2007;**53**:506—13.

24. De Coppi P, Bellini S, Conconi MT, et al. Myoblast-acellular skeletal muscle matrix constructs guarantee a long-term repair of experimental full-thickness abdominal wall defects. *Tissue Eng* 2006;**12**:1929—36.

25. Marzaro M, Conconi MT, Perin L, et al. Autologous satellite cell seeding improves in vivo biocompatibility of homologous muscle acellular matrix implants. *Int J Mol Med* 2002;**10**:177—82.

26. Warren GL, Ingalls CP, Shah SJ, Armstrong RB. Uncoupling of in vivo torque production from EMG in mouse muscles injured by eccentric contractions. *J Physiol* 1999;**515**(Pt 2):609—19.

27. Gamba PG, Conconi MT, Lo Piccolo R, et al. Experimental abdominal wall defect repaired with acellular matrix. *Pediatr Surg Int* 2002;**18**:327—31.

28. Willett NJ, Li MT, Uhrig BA, et al. Attenuated rhBMP-2 mediated bone regeneration in a rat model of composite bone and muscle injury. *Tissue Eng Part C Methods* 2012;**19**(4):316—25.

29. Turner NJ, Badylak JS, Weber DJ, Badylak SF. Biologic scaffold remodeling in a dog model of complex musculoskeletal injury. *J Surg Res* 2011;**176**(2):490—502.